Title

Coupled THMC models for bentonite in an argillite repository for nuclear waste: Illitization and its effect on swelling stress under high temperature

Authors

Zheng, Liange

Rutqvist, Jonny

Xu, Hao

et al.

Publication Date

2017-11-01

DOI

10.1016/j.enggeo.2017.10.002

Peer reviewed

Coupled THMC models for bentonite in an argillite repository for nuclear waste: Illitization and its effect on swelling stress under high temperature

Liange Zheng, Jonny Rutqvist, Hao Xu, Jens T. Birkholzer

Abstract

Subsurface manipulations such as those expected from the disposal of heat-emanating radioactive waste in deep repositories can induce strongly coupled Thermal (T), hydrological (H), mechanical (M) and chemical (C) processes. Adequate coupled THMC models are highly desirable or even indispensable for performance assessment of such repositories, for examples for the analysis of bentonite-based engineered barrier system (EBS) surrounding the emplaced waste. In this study, we present coupled THMC model simulations of a generic nuclear waste repository in an argillite with a bentonite-based buffer. The objective is to evaluate the chemical changes in the EBS bentonite and their effect on mechanical behavior under high temperature, attempting to shed light on whether EBS bentonite can sustain temperatures higher than 100 °C without significant impact on barrier's performance.

Two scenarios were simulated for comparison: a case in which the temperature near the waste canister peaks at 200 °C and a case in which the temperature at the same spot culminate with about 100 °C. Simulations for a generic case with Kunigel-VI bentonite as backfill and Opalinus Clay as host rock were conducted for 1000 years and reported in the previous study (Zheng et al., 2015). In this paper, simulations for 100,000 years have been done for two types of bentonite-based buffer materials: Kunigel-VI and FEBEX bentonite. This enables us to evaluate how different types of bentonite behave in terms of the illitization and its impact on swelling stress and whether we can generalize these results to support decision making. The simulations show the occurrence of illitization in the bentonite buffer and the enhancement of illitization under high temperature. However, FEBEX bentonite undergoes less illitization mainly due to the higher ion concentration in pore water and the lower content of K-feldspar in the bentonite mineral composition. Moreover, the reduction of swelling stress by

chemical changes is more pronounced for Kunigel-VI bentonite than for FEBEX bentonite. Overall, the results of our model simulations suggest that an argillite repository with a bentonite-based EBS that is similar to FEBEX bentonite could sustain temperatures much higher than 100 °C as far as illitization concerns. Model results also reveal that illitization is stabilized after about 2000 years in bentonite near the waste package, but continues in bentonite near the bentonite-argillite interface, which manifests the strong effect of geochemical interaction between EBS bentonite and host rock on long term illitization in bentonite.

1. Introduction

Numerical models are important tools in evaluating various subsurface engineering activities such as CO_2 geological sequestration, geological disposal of radioactive nuclear waste, oil/gas production, and acid gas injection. The application of such models requires thorough understanding of the evolution of thermal (T), hydrological (H), mechanical (M) and chemical (C) processes during the practice of these activities. Although these processes have certain degrees of independence and can be simulated individually (without considering coupling with other processes) under certain conditions, it is in many cases necessary to consider the interactions between different processes. Some obvious and important couplings are TC (the effect of temperature on chemical reactions), HC (the effect of transport on chemical reactions), TM (the effect of temperature on mechanical deformation and stress), and HM (the effect of fluid pressure on mechanical deformation and stress) couplings. In the last decades, numerous THM as well as THC model have been developed and applied to a wide range of applications. Recently, fully coupled THMC models have also been developed to accommodate the coupling between chemical and mechanical processes on top of THC and THM interactions. For example, Yin et al. (2010) presented a fully coupled THMC model for studying wellbore stability during oil/gas production; Yin et al. (2011)further applied their THMC model to injection of CO_2 into a carbonate aquifer, whereas Zhang et al. (2012) developed a coupled THMC model for CO_2sequestration in brine aquifers. Moreover, THMC models have also been developed with application for modeling geothermal systems (Taron et al., 2009, Kim et al., 2015).

Geological disposal of radioactive nuclear waste is an area in which coupled THMC models have been actively pursued in recent years. The DECOVALEX-THMC project (Tsang, 2009) is a one example of such an effort, which included studies related to coupled THC and THM processes around nuclear waste emplacement tunnels in granite and tuff host rocks, but did not fully address full THMC couplings. THMC models have increasingly been used in studying the evolution of bentonite in the engineered barrier system (EBS) and clay-rich host rock due to the close interaction of chemical and mechanical processes therein. This includes a series of THMC models (Guimarães et al., 2007, Zheng and Samper, 2008, Zheng et al., 2010, Zheng et al., 2011) that were developed associated with the FEBEX project (ENRESA, 2000) to study the evolution within FEBEX bentonite and other models for similar type of bentonite (Gens et al., 2004, Guimarães et al., 2013, Rutqvist et al., 2014, Zheng et al., 2014).

An engineered barrier system (EBS) that includes a bentonite-based buffer is widely used in the multi-barrier system designs for geological disposal of radioactive waste throughout the world. Argillite is one of the candidate host rocks that have been extensively studied in various countries, especially in Europe. The maximum temperature to which the EBS and host rock can safely withstand is one of the most important design variables for a geological repository, because it determines waste package spacing, distance between disposal galleries, and therefore the overall size (and cost) of a repository for a given amount of heat-emanating waste (Horseman and McEwen, 1996). This is of particular importance for an argillite repository, because argillite has relatively lower heat conductivity. All disposal concepts throughout the world, despite their differences in design concepts, commonly impose an upper temperature limit of about 100 °C (Hicks et al., 2009). Chemical alteration and the subsequent changes in mechanical properties are among the determining factors. A higher temperature could result in chemical alteration of bentonite-based buffer and backfill materials within the EBS through illitization and cementation, which compromise the function of these EBS components by reducing their plasticity and capability to swell under wetting (Pusch and Karnland, 1996, Pusch et al., 2010, Wersin et al., 2007). The swelling capability of bentonite is important for sealing gaps between bentonite blocks, between bentonite and other EBS components, and between the EBS and the surrounding host rock. Chemical

alteration may also occur in the near-field argillite, which could inhibit the self-sealing within the excavation damaged zone (EDZ). Because the permeability of clay rock is low, a higher temperature may also induce significant pore pressure build-up in the near field, which could generate adverse mechanical deformation (such as fracturing), damaging the integrity of the host rock (Horseman and McEwen, 1996).

Regarding the concern of chemical alteration and the associated mechanical changes, Wersin et al. (2007) concluded that the criterion of 100 °C for the maximum temperature within the bentonite buffer is overly conservative. In another review, Zheng et al. (2015) concurred with the conclusion of Wersin et al. (2007), i.e. that the 100 °C temperature limit on bentonite may likely be unwarranted. Specifically, Zheng et al. (2015) noted that the impact of a high temperature on bentonite and clay rock behavior are largely open questions for a argillite repository system and that coupled models are needed that integrate the relevant THMC processes and consider the interaction between EBS and host rock.

In an attempt to shed some light on the issue of high temperature limit, coupled THMC models were developed in Liu et al. (2013) and Zheng et al. (2015) and applied for studying a generic repository case involving a bentonite-base buffer in the EBS hosted in a clay rock formation. It was assumed that the EBS bentonite was Kunigel-VI bentonite (Ochs et al., 2004) and that the host rock properties were representative of Opalinus Clay (Bossart, 2011, Lauber et al., 2000). The 1000-year simulations in Zheng et al. (2015) showed that illitization was enhanced under high temperature and resulted in a notable reduction in swelling stress in EBS bentonite. However, questions arise if such findings still hold for other type of bentonite and for much longer simulation time, i.e. 100,000 years. Among a variety of bentonite types that have been studied as EBS material throughout the world, the Kunigel-VI bentonite (Ochs et al., 2004) has very low smectite content and consequently a relatively low swelling capacity. In this paper, we first present THMC modeling of Kunigel-VI bentonite with expanded simulation time to 100,000-years, and then THMC modeling was conducted for FEBEX bentonite, which is very distinct from Kunigel-VI bentonite—it has a much higher fraction of smectite and swelling capacity. Our objectives are to study when the illitization will be stabilized and evaluate how different types of bentonite behave in terms of illitization and

subsequent stress under high temperature, and whether we can generalize these results to support decision making.

2. The THMC simulator

Over last decade, some THC or THM codes have also been expanded to consider various types of THMC processes, such as versions of CODE_BRIGHT (Guimarães et al., 2007, Guimarães et al., 2013); FADES-CORE (Zheng and Samper, 2008) and TOUGH2-CSM (Zhang et al., 2012), TR-FLAC (Taron et al., 2009), TOUGHREACT-FLAC (Zheng et al., 2015), and TOUGHREACT-ROCMECH (Kim et al., 2015). The OPEN-GEOSYS (Wang et al., 2011) and MOOSE (Gaston et al., 2009) model frameworks are open and flexible software environments that allow coupling of THMC processes. Consideration of the coupling between chemistry and mechanics differs depending on the application, e.g. geothermal versus nuclear waste disposal, and various simplifications have been employed in order to focus on relevant couplings and processes for the specific problem to be solved.

The simulations in this paper were conducted with TOUGHREACT-FLAC3D, which integrates TOUGH-FLAC (Rutqvist et al., 2011) and TOUGHREACT Version 2 (Xu et al., 2011). It included a linear elastic swelling model to account for swelling as a result of changes in saturation and pore-water composition and the abundance of swelling clay (Zheng et al., 2015). Fig. 1 shows the coupling scheme of TOUGHREACT-FLAC3D. In each time step, TOUGHREACT calculates the primary variables for THC processes including temperature (T), liquid pressure (P_l) or gas pressure (P_g), water saturation (S_l), ion concentrations of pore water (C_i) and concentration of exchangeable cations and/or abundance of swelling clay minerals (X_i). These primary variables are then passed to FLAC3D via a coupling module to conduct stress and strain analysis. The coupling between THC processes (provided by TOUGHREACT) and the mechanical part (FLAC3D) is carried out at every time step. Because the strongly coupled THC processes simulated in TOUGHREACT can lead to very small time steps and sequentially invoking the FLAC3D stress and strain analysis can consume a large portion of the total computation time, a time step management scheme was implemented in TOUGHREACT-FLAC3D. A subroutine was inserted in TOUGHREACT to check the change of primary variables from the previous time step and decide if the change is large enough to warrant an update in stress/strain

based on the predetermined criteria. The choice of criteria is arbitrary. After testing several values, a criterion of 1–2% change in primary variable was selected that reduces computation time significantly and ensures that the calculated stress is very close (within 0.1% difference) to that obtained by updating stress/strain every time step.

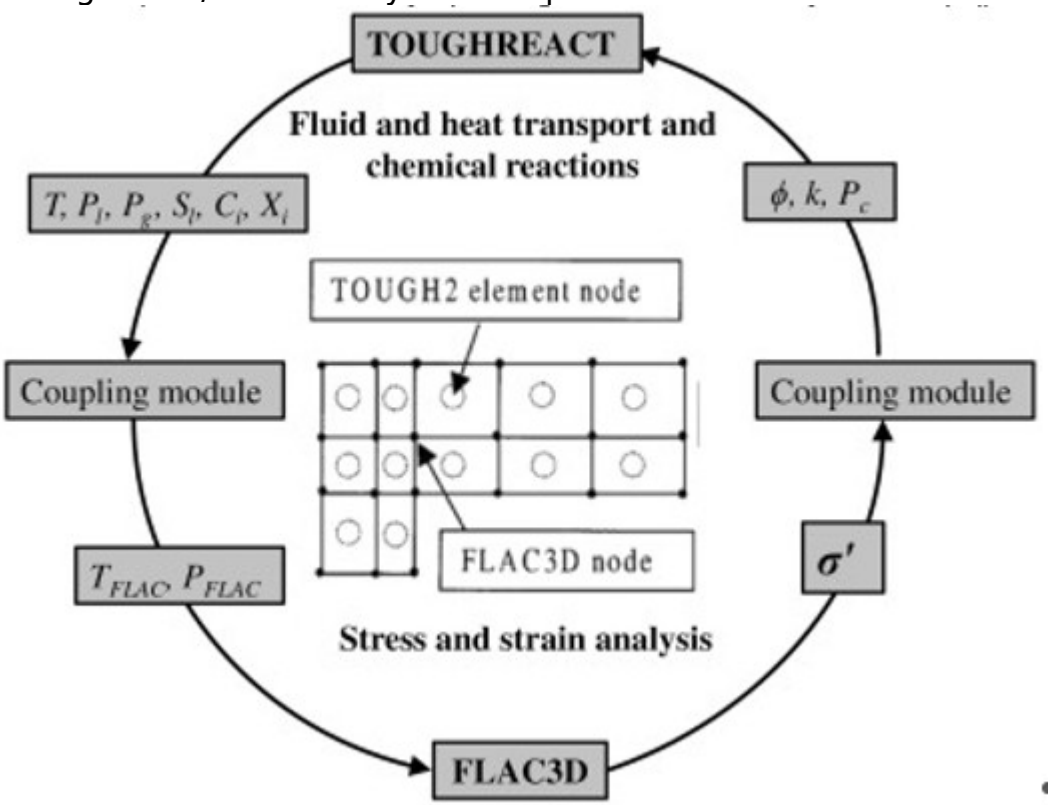

Fig. 1. The coupling scheme for TOUGHREACT-FLAC3D.

3. Model development

3.1. Modeling scenario

Here we briefly describe the THMC modeling scenario, whereas additional details are presented in Zheng et al. (2015). The model is applied to a hypothetical bentonite-backfilled nuclear waste repository in argillite at 500 m depth (Fig. 2) (Rutqvist et al., 2014). The *Z*-axis is the vertical direction, while the horizontal Y- and X-axes are aligned parallel and perpendicular to the emplacement tunnel, respectively (Fig. 2) in this 2-D model.

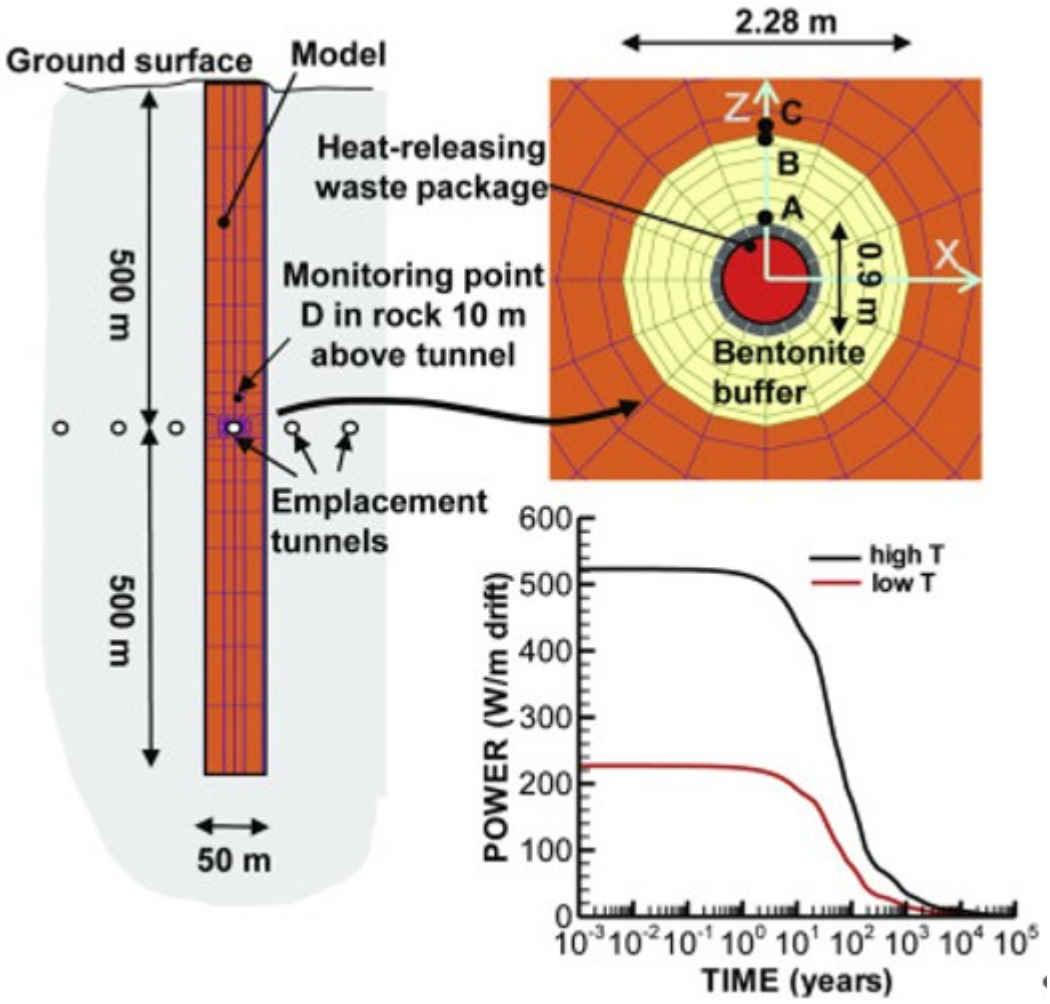

Fig. 2. Domain for the test example of a bentonite back-filled horizontal emplacement drift at 500 m (Rutqvist et al., 2014). Modeling monitoring points: A: inside the bentonite near the canister, B: inside the bentonite and near the bentonite-argillite interface, C: inside the clay rock formation and near the bentonite-argillite interface, D: inside the argillite at a distance of 10 m from the canister. “High T”: 200 °C; “Low T”: 100 °C.

An initial stress field is prescribed according to the self-weight of the rock mass. Zero normal displacements are applied on the lateral boundaries, whereas zero stress is prescribed to the top and vertical displacements are prevented at the bottom. An open boundary is applied to the liquid pressure at the top and bottom and initially the model domain is hydrostatic. The initial temperature is about 11 °C at the top and 38 °C at the bottom, corresponding a thermal gradient of 27 °C/km. The model simulation was nonisothermal with a time-dependent heat power input (Rutqvist et al., 2014). Initially the EBS bentonite has a water saturation of 65% and the argillite is fully saturated. From time zero, the EBS bentonite undergoes

simultaneously re-saturation, heating, chemical alteration, and stress changes.

3.2. Chemo-mechanical model

Details of the mechanical model implemented in the TOUGHREACT-FLAC3D are given in Rutqvist et al. (2014). Here we briefly describe the mechanical models for the EBS bentonite and argillite. For nonisothermal behavior of unsaturated soils, we may partition the total incremental strain into elastic (ε^e), plastic (ε^p), suction (ε^s), thermal strains (ε^T) and chemical strains (ε^c):

(1)dε=dεe+dεp+dεs+dεT+dεc

where the suction strain represents the strain associated with changes in suction and chemical strain represents the strain associated with change in chemical conditions, including changes in ion concentration and abundance of swelling clay mineral Each of these types of strain, except chemical strain, is described in Rutqvist et al. (2014).

Similar to thermally induced strains, chemical strains are purely volumetric:

(2)dεc=−An∗dC+Asc∗dMs

where A_n^* is a constant that linearly relates ion concentration (C) variation and the corresponding strain change. A_{sc}^* is a constant that relates the change in mass fraction of swelling clay, $Ms.$, to change in strain.

A linear elastic swelling model essentially defines the suction strain as a function of water saturation:

(3)dεs=βswdSl

where Sl is the water saturation and β_{sw} is a moisture swelling coefficient. Under mechanically constrained conditions and considering the linear relationship between swelling stress and suction strain, $d\sigma_s = 3Kd\varepsilon^s$, we have a swelling stress that is linearly proportional to the saturation:

(4)dσs=3KβswdSl

where K is the bulk modulus. Eq. (3) is what was used for EBS bentonite in a so-called simple swelling approach in Rutqvist et al. (2011), whereas the final stress induced by the swelling depends on the degree of confinement, with the maximum possible swelling stress obtained from Eq. (4). In this paper, β_{sw} is 0.238, calibrated using the swelling pressure of 5 MPa for FEBEX bentonite (Castellanos et al., 2008) under the condition that bentonite is saturated with dilute solution (e.g. deionized water), and K is 20 MPa (Rutqvist et al., 2011).

To consider the swelling due to both moisture and chemical changes, we include the stress due to a change of ion concentration in the pore water and abundance of swelling clay:

(5)dσs=3Kdεs+dεc=3KβswdSl+An∗dC+Asc∗dMs=3KβswdSl+AndC+AscdMs

where $A_n = 3KA_n^*$ is a constant that linearly relates ion concentration (C) variation and the corresponding swelling stress change. $A_{sc} = 3KA_{sc}^*$ is a constant that relates the change in mass fraction of swelling clay, *Ms.*, to change in swelling stress. Eq. (5) expresses the maximum swelling stress that could occur under fully constrained mechanical conditions, while the actual stress developed in the calculation depends on the degree of confinement at each local point in the model domain.

A_n is typically calculated from swelling pressures measured using different solutions (e.g. deionized water versus 1 M NaCl solution) to saturate the bentonite. Laredj et al. (2010) proposed the following expression for A_n:

(6)An=5.312InC−23.596C−7.252×10−4C2

An empirical value for A_{sc} is derived through a linear regression of swelling pressure versus smectite mass fractions (Zheng et al., 2015). A_{sc} for Kunigel VI bentonite is 2.5×10^6 Pa whereas for FEBEX A_{sc} is 6.5×10^6 Pa.

More sophisticated and realistic mechanical models are available in the literature and have been successfully used for bentonite and argillites, such as the state surface approach (e.g., Nguyen et al., 2005) and the dual structure Barcelona Expansive Clay model (Alonso et al., 1999, Sánchez et al., 2005). In this paper, we use a rather simple elastic model because it allows us to incorporate the contribution from the chemical components and parameters and the model can be relatively easily calibrated as discussed above.

For argillites, we extend the elastic model used in Rutqvist et al. (2014) to consider the chemical strain as in Eq. (2). The parameters, A_n and A_{sc}, are same as those used for bentonite, with an assumption that compacted bentonite and clay rock behave similarly in terms of the effect of chemical change on strain. However, the validity of this assumption needs to be confirmed with more data.

3.3. Chemical and hydrological model

In these generic cases, it is assumed that that the properties of the argillite are representative of Opalinus Clay (Bossart, 2011, Lauber et al., 2000). For

the EBS bentonite, Zheng et al. (2015) used Kunigel-VI bentonite (Ochs et al., 2004) and in this paper FEBEX bentonite (ENRESA, 2000) is also used. The mineral compositions of the bentonite and argillite are listed in Table 1. The pore-water compositions of the Kunigel-VI bentonite (Sonnenthal, 2008), FEBEX bentonite (Fernández et al., 2001) and the argillite (Fernández et al., 2007) are listed in Table 2. Table 3 lists the thermal, hydraulic and mechanical material parameters used in the model.

Table 1. Mineral volume fraction (dimensionless, ratio of the volume for a mineral to the total volume of medium) of the Kunigel-VI bentonite (Ochs et al., 2004), FEBEX bentonite (ENRESA, 2000, Fernández et al., 2004, Ramírez et al., 2002) and Opalinus Clay (Bossart, 2011, Lauber et al., 2000).

Mineral	EBS bentonite: Kunigel-VI	EBS bentonite: FEBEX	Argillite: Opalinus clay
Calcite	0.016	0.0065	0.093
Dolomite	0.018	0.0	0.050
Illite	0.000	0.0	0.273
Kaolinite	0.000	0.0	0.186
Smectite	0.314	0.6	0.035
Chlorite	0.000	0.0	0.076
Quartz	0.228	0.026	0.111
K-Feldspar	0.029	0.0065	0.015
Siderite	0.000	0.0	0.020
Ankerite	0.000	0.0	0.045

Table 2. Pore-water composition (mol/kg water, except pH) of Kunigel-VI bentonite(Sonnenthal, 2008), FEBEX bentonite (Fernández et al., 2001) and Opalinus Clay (Fernández et al., 2007).

	EBS bentonite: Kunigel-VI	EBS bentonite: FEBEX	Argillite: opalinus clay
pH	8.40	7.72	7.40

	EBS bentonite: Kunigel-VI	EBS bentonite: FEBEX	Argillite: opalinus clay
Cl	1.5×10^{-5}	1.6×10^{-1}	3.32×10^{-1}
SO_4^{-2}	1.1×10^{-4}	3.2×10^{-2}	1.86×10^{-2}
HCO_3^-	3.49×10^{-3}	4.1×10^{-4}	5.18×10^{-3}
Ca^{+2}	1.37×10^{-4}	2.2×10^{-2}	2.26×10^{-2}
Mg^{+2}	1.77×10^{-5}	2.3×10^{-2}	2.09×10^{-2}
Na^+	3.6×10^{-3}	1.3×10^{-1}	2.76×10^{-1}
K^+	6.14×10^{-5}	1.7×10^{-3}	2.16×10^{-3}
Fe^{+2}	2.06×10^{-8}	2.06×10^{-8}	3.46×10^{-6}
SiO_2(aq)	3.38×10^{-4}	1.1×10^{-4}	1.1×10^{-4}
AlO_2^-	1.91×10^{-9}	1.91×10^{-9}	3.89×10^{-8}

Table 3. THM parameters.

Parameter	Argillite: Opalinus clay	EBS bentonite
Grain density [kg/m³]	2700	2700
Porosity ϕ	0.162	0.33
Saturated permeability [m²]	2.0×10^{-20}	2.0×10^{-21}
Relative permeability, k_{rl}	$m = 0.6$, $S_{rl} = 0.01$	$K_{rl} = S^3$
Van Genuchten α [1/Pa]	6.8×10^{-7}	3.3×10^{-8}
Van Genuchten m	0.6	0.3
Compressibility, β [1/Pa]	3.2×10^{-9}	5.0×10^{-8}
Thermal expansion coeff., [1/°C]	1.0×10^{-5}	1.5×10^{-4}
Dry specific heat, [J/kg-°C]	860	800
Thermal conductivity [W/m- C] dry/wet	1.48/1.7[a]	0.5 1.3
Tortuosity for vapor phase	ϕ1/3Sg10/3	ϕ1/3Sg10/3
Bulk modulus, (GPa)	4.17	0.02
Shear modulus, (GPa)	1.92	0.0067

a

From http://www.mont-terri.ch/internet/mont-terri/en/home/geology/key_characteristics.html
FEBEX and Kunigel-VI bentonite also have distinct hydrological and thermal parameters, with the most relevant ones being thermal conductivity and permeability. However, in this paper, we use the same thermal conductivity and permeability for both bentonites. These parameters are actually fairly similar for the two types of bentonite — thermal conductivity for saturated Kunigel-VI bentonite is 1.5 W/m-°C and that for FEBEX bentonite is 1.3 W/m °C (ENRESA, 2000); permeability for Kunigel-VI bentonite is 2E-21 m^2 and that for FEBEX ranges from 1×10^{-21} to 3.75×10^{-21} m^2 (ENRESA, 2000, Zheng et al., 2011, Chen et al., 2009). Moreover, by using the same values of thermal conductivity and permeability for both bentonites, we can isolate the effect of variations in chemical and CM coupling parameters on the stress changes.
Mineral dissolution/precipitation is kinetically controlled. The kinetic law for mineral dissolution/precipitation is given in Xu et al. (2011) and the kinetic rates and surface areas for the minerals considered in the model were given in Zheng et al. (2015).

3.4. Model limitations

Because the problem we are dealing with in this paper is very complex and developing fully coupled THMC models is challenging, simplifications are made for programatic purpose. First, the canister serves only as a heat source; chemical changes on the surface of the canister are neglected. Further model analysis is warranted to consider chemical interaction between canister and bentonite. Second, the mechanical-chemical coupling is calculated using an extended linearly elastic swelling submodel in which key parameters are empirical. A more rigorous and theatrically-based approach linking chemistry and mechanics might leads to different model results. Third illitization is simulated as a dissolution-precipitation process, i.e., the dissolution of smectite and neo-formation of illite, with the illitization rate calibrated against field data (Pusch and Madsen, 1995). It is known that illitization could also occur through solid state transformation by substitution of intracrystal cations (e.g., Cuadros and Linares, 1996), which is not considered in our model. However, the chemical reaction for illitization via solid state transformation is still a matter of debate and the appropriate

reaction rate is a large uncertainty, which prevents us from incorporating this mechanism in the model. Last but not least, in current chemical model, only abiotic reactions are considered and microbiological activities are ignored. However, biochemical reactions affect the evolution of pH and Eh and subsequently may impact illitization as well. In the future, more comprehensive chemical model that includes biochemical reactions is warranted.

4. Model results

In Liu et al. (2013) and Zheng et al. (2015), the model results for the first 1000 years, expressed as the evolution of temperature, pore pressure, water saturation, concentration and stress, were discussed in detail and a sensitivity analysis to key chemical and mechanical parameters were conducted to understand the coupling processes. The simulations were only conducted for a period of 1000 years because the older version of TOUGHREACT-FLAC3D was not fast enough for longer simulation time periods and because it was expected that coupled process effects are most pronounced in the first 1000 years. One of the general observations based on these simulations is that illitization is enhanced at higher temperature, although the amount of illitization depends on chemical and hydrological conditions and varies a great deal. These results lead to questions about illitization at longer times (i.e., 100,000 years). For example, does illitization continue at the same rate or does it stabilize at long times and how does illitization affect stress at longer times? In this paper, we have been able to address these questions with the improved version of TOUGHREACT-FLAC3D, which can carry out simulations to 100,000 years.

4.1. Cases for Kunigel-VI bentonite

In the generic cases we used to study the effect of high temperature on the THMC evolution in the bentonite buffer and argillite, two bentonites have been simulated: Kunigel-VI and FEBEX bentonite. In this section, model results for Kunigel-VI bentonite are presented. We first briefly discuss the changes in temperature, water saturation and the volume fraction of smectite because their changes essentially determine the evolution of stress; then the changes in stress are discussed.

4.1.1. THC evolution

The heat release rates have been adjusted to make two cases for comparison: a “high T” case, in which the temperature near the canister can reach 200 °C; and a “low T” case, in which the temperature near the canister peaks at about 100 °C. In this paper, the temporal evolution at the four monitoring points (shown in Fig. 2) is used to present thermal, hydrological, chemical and mechanical results: point A is inside the bentonite near the canister, point B is inside the bentonite near the bentonite-argillite interface, point C is inside the argillite near the bentonite-argillite interface, and point D is inside the argillite at a distance of 10 m from the canister. After 100,000 years, the temperature drops to about 27 °C (Fig. 3). As expected the bentonite gradually becomes fully saturated and interestingly desaturation occurs in the argillite because the host rock is not able to replenish water as fast as it is being imbibed by the EBS bentonite. It takes about 20 years for the bentonite become fully saturation for the ‘low T’ case and 25 years for “high T” case. Pore pressure increases as a result of re-saturation and heating. The “high T” case exhibits much higher pore pressure than the “low T”, with a difference of about 5 MPa after 1000 years, but by the end of 100,000 years, the difference is fairly small. Details of water saturation and pore pressure evolution can be found in Zheng et al. (2015).

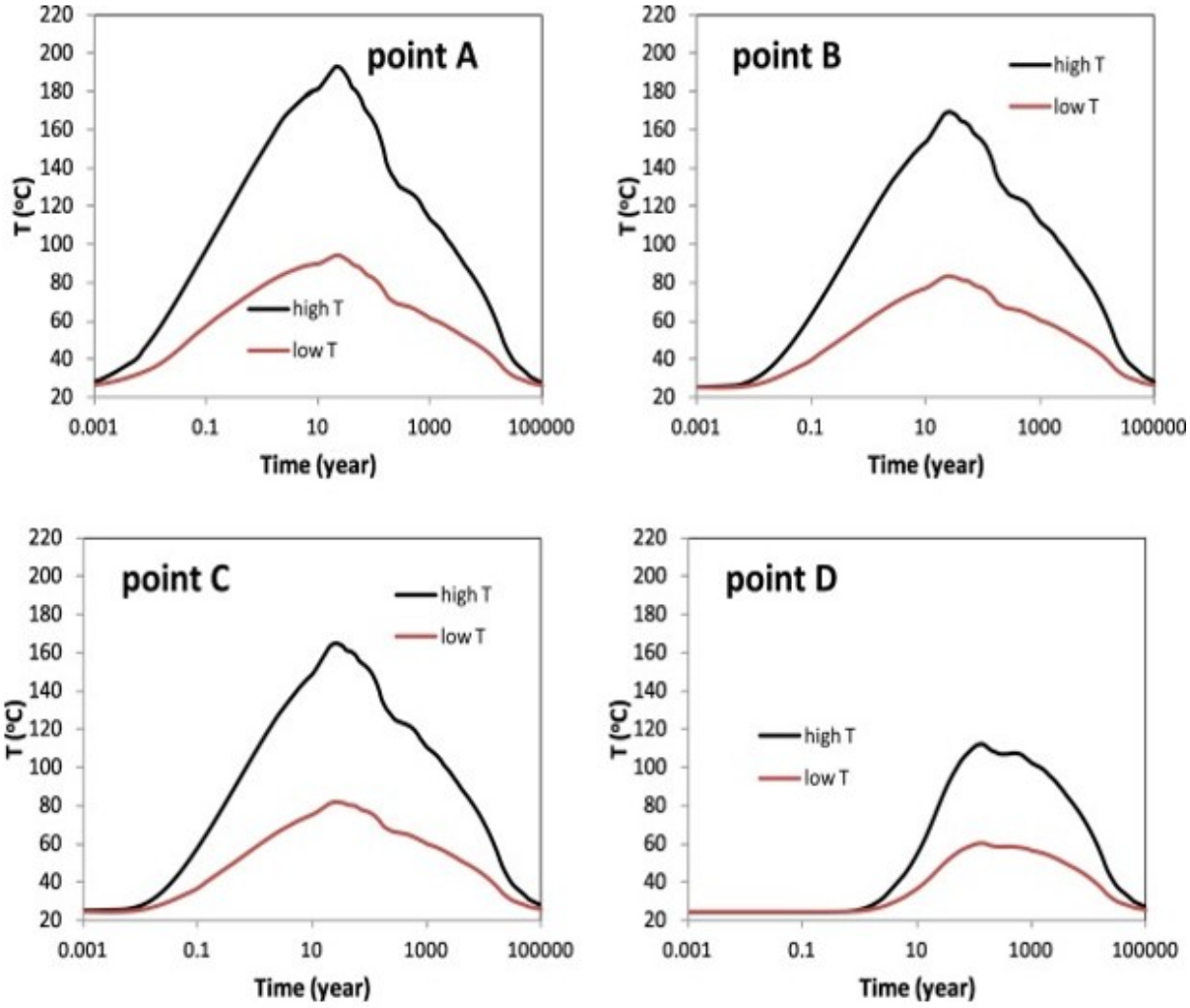

Fig. 3. Temperature evolution at points A, B, C, and D.

In the model, illitization is modeled as the dissolution of Na-smectite and precipitation of illite. As shown by THC modeling in Liu et al. (2013) and Zheng et al. (2015), many factors can affect the chemical reactions such as the initial water-mineral disequilibrium in bentonite (since the water used for making bentonite blocks is not necessarily in equilibrium with the mineral phase in bentonite, and it takes time to reach that equilibrium), as well as the thermal and hydrological disturbances in response to emplacement.

Smectite volume fraction changes at points A through D are shown in Fig. 4; illite volume fraction changes are shown in Fig. 5. Consistent with the model in Zheng et al. (2015), illitization does occur in the EBS bentonite. In addition to temperature effects, illitization is affected by the initial disequilibrium

between the pore-water solution and mineral phases, interaction between EBS bentonite and argillite. Note that the increase in Al and K concentrations in bentonite is the key to initiate the illitization and it is caused not only by diffusion and advection, but also by the dissolution of other minerals, such as K-feldspar. After 1000 years (the simulation time of previous models in Zheng et al., 2015) the smectite volume fraction in the bentonite decreases by 0.035 (or 11%) for the 'high T" case and 0.006 (or 2%) for the "low T" case, which corresponds to an illite volume fraction increase of similar magnitude. Smectite volume fraction changes are similar at point A and B. However, after 2,000 years, illitization exhibits distinct behavior at points A and B for the "high T' case. At point A, illitization is stagnant, which would be more clearly illustrated if Fig. 4 is plotted on a linear scale. This is mainly caused by the drop of temperature, which significantly slowed down the dissolution of K-feldspar and subsequently the supply of K. The reduced temperature also significantly decreases the reaction rate of smectite and illite. Conversely, at point B, the illitization in bentonite continues at fairly fast rate due to the interaction with argillite. Although the dissolution rate of K-feldspar at point B is significantly reduced (which limits the supply of K), bentonite near the bentonite-argillite interface receives K from the argillite. This source of K is depleted before 2000 years by illitization in the argillite. However, illitization ceases in the argillite after 2000 years such that K is free to move into the bentonite. After 100,000 years, for the "high T" case, at point A, smectite volume fraction decreases by about 0.05, equivalent to 17% of the initial amount of smectite, while at point B, smectite volume fraction decreases by about 0.19, close to 60% of the initial amount of smectite. The difference between the illitization at points A and B shows that without interaction with host rock, the thermal-induced chemical alteration in the EBS bentonite stabilizes after 2000 years (e.g. results at point A), but the interaction with host rock may lead to dramatic changes in bentonite as illustrated by the model results at point B. For the "low T", smectite volume fraction decreases by about 0.03 (10% of initial amount) at points A and B after 100,000 years, which is substantially lower than that for "high T' case, especially at point B.

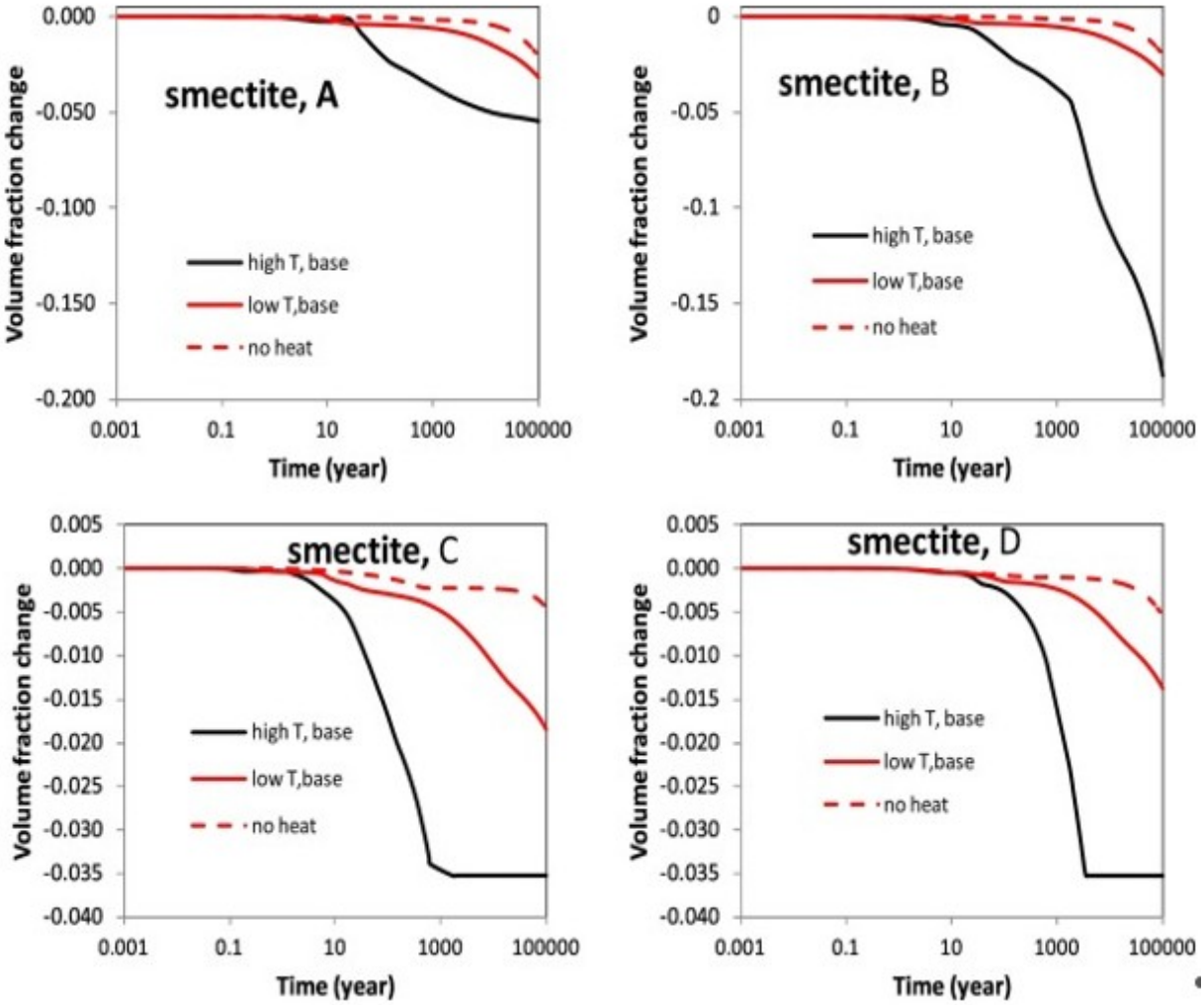

Fig. 4. The temporal evolution of smectite volume fraction at points A, B, C, and D.

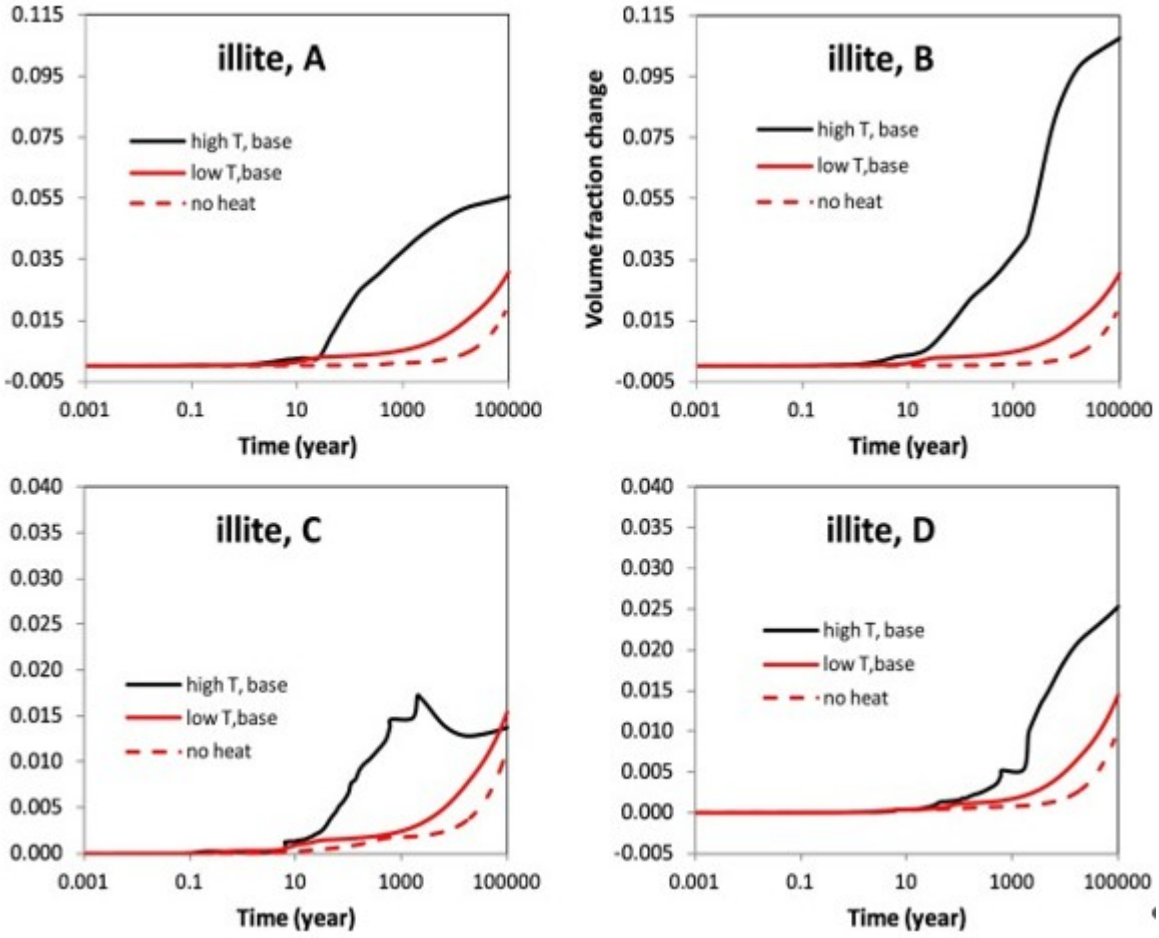

Fig. 5. The temporal evolution of illite volume fraction at points A, B, C, and D.

In Fig. 4, Fig. 5, model results are also shown for a simulation (“no heat”) that assumes there is no heat release from waste package. This simulation illustrates that the chemical alteration in EBS bentonite is caused mostly by the interaction between bentonite and argillite. Even though there is no temperature increase, Kunigel-VI bentonite tends to undergo slight illitization which results in a decrease of smectite volume fraction of 0.02 (5% of the initial amount) in 100,000 years.

Results from Fig. 4, Fig. 5 confirm that the argillite undergoes a small degree of illitization similar to observations in geological systems (e.g. Wersin et al., 2007, Pusch and Madsen, 1995).This is illustrated by the smectite dissolution at points C and D in Fig. 4 and illite precipitation at points C and D in Fig. 5. Results at point D represent the chemical alteration in the argillite induced only by the long term heating. The volume fraction of smectite in the argillite, which initially is 0.035, is depleted after 3500 years for the “high T”

case and decreases by 0.0135 (about 40% of initial amount) for the “low T” case in 100,000 years. As a comparison, the “no heat” simulation shows that argillite undergoes a decrease in smectite volume fraction of 0.005 (14% of the initial amount) for undisturbed temperature conditions. At point C near the bentonite-argillite interface, because the argillite undergoes interaction with bentonite and experiences higher temperature, illitization is faster in comparison with that at point D. For the “high T” case, in only 650 years, the volume fraction of smectite decreases by 0.034 (about 97% of initial amount) and then in about 1500 years, all smectite is transformed to illite; for the “low T” case, the volume fraction of smectite decreases about 0.017 (50% of the initial amount) in 100,000 years. As mentioned above, the quick depletion of smectite or the cessation of illitization in the argillite near the bentonite-argillite interface has significant impact on the illitization in bentonite. In the “no heat” simulation, the model result at point D represents the chemical evolution for undisturbed temperature conditions — which shows a slow illitization in the argillite, with a decrease of smectite volume fraction about 0.005 in 100,000 years.

4.1.2. Stress evolution

The mechanical-chemical coupling implemented in the current model allows us to evaluate how the chemical changes described in Section 4.1.1 may affect the mechanical behavior of the EBS bentonite in terms of swelling and total stress. We limit our analysis to the effects of ion concentration and illitization on swelling and do not include other potential effects of chemical changes on mechanics, such as changes in mechanical properties due to cementation.

Fig. 6, Fig. 7 show the stress changes at point A and B for both “low T” and “high T” cases. Several processes combine to drive the peak stress in bentonite up to about 5 MPa for the “low T” case and 13 MPa for the “high T” case, both at around 100 years. Reasons for the stress increase include the increase in pore pressure due to hydration and thermal pressurization (a processes caused by the difference in thermal expansion of the fluid and solid host rock), bentonite swelling, and thermal expansion. Clearly the stronger thermal pressurization in the “high T” case leads to much higher stress in the bentonite than the “low T” case. For both the “high T” and “low T” cases, the major contribution to total stress within the buffer is pore

pressure, with smaller contributions from swelling and thermal stresses. After 100 years, the stress gradually goes down and stabilizes somewhat after 30,000 years. By the end of 100,000 years, the difference between the “high T” and “low T” cases is minimal.

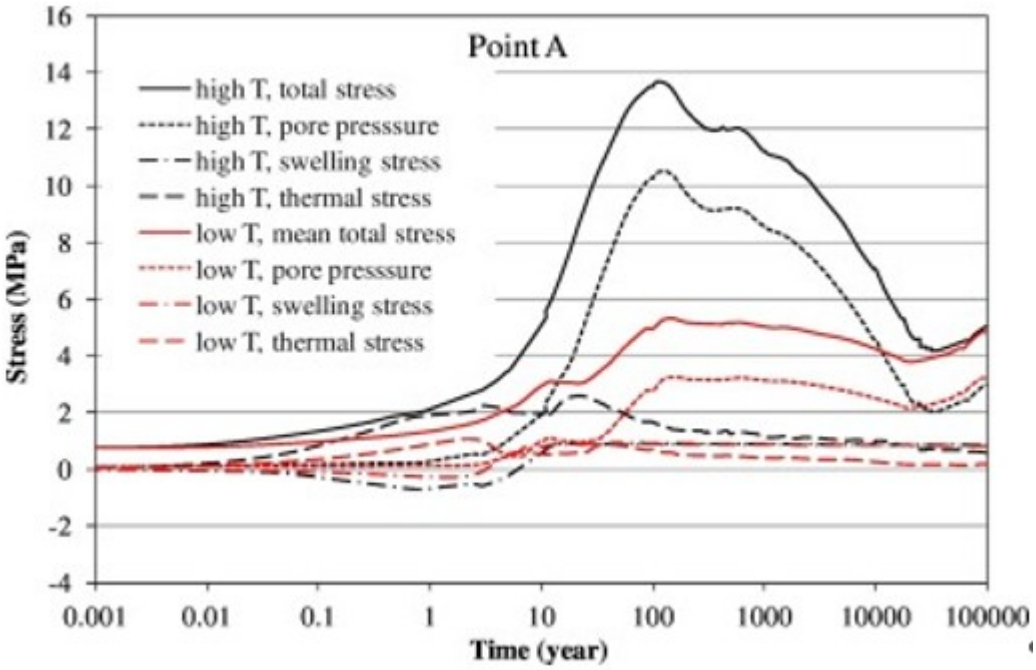

Fig. 6. Simulation results of mean total stress, pore pressure, and thermal stress at point A for the “low T” and “high T” scenario, respectively.

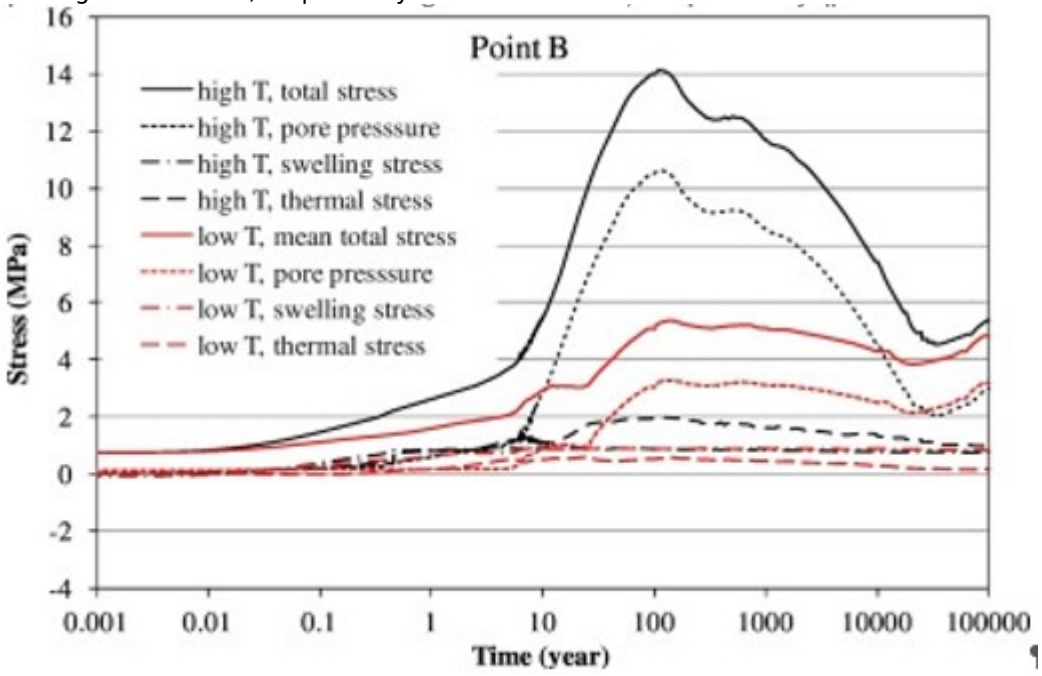

Fig. 7. Simulation results of mean total stress, pore pressure, and thermal stress at point B for the “low T” and “high T” scenario, respectively.

The constitutive relationship described by Eq. (5) provides an opportunity to evaluate the effect of chemical changes on swelling stress. In order to isolate the contributions of ion concentration changes versus smectite changes on swelling stress changes, we present three sets of calculated swelling stress. In the first set, denoted in Fig. 8, Fig. 9 as “σ = f(Sl,C,Ms)”, the swelling stress is calculated according to Eq. (5) as a function of liquid saturation changes (Sl), ion concentration (C) changes, and smectite (Ms) changes. In the second set, denoted as “σ = f(Sl,C)”, the contribution from smectite changes in Eq. (5) is disregarded, and the swelling stress is only a function of liquid saturation and ion concentration. In the third set, denoted as “σ = f(Sl)”, all chemical effectsare neglected, and the swelling stress is only a function of liquid saturation changes.

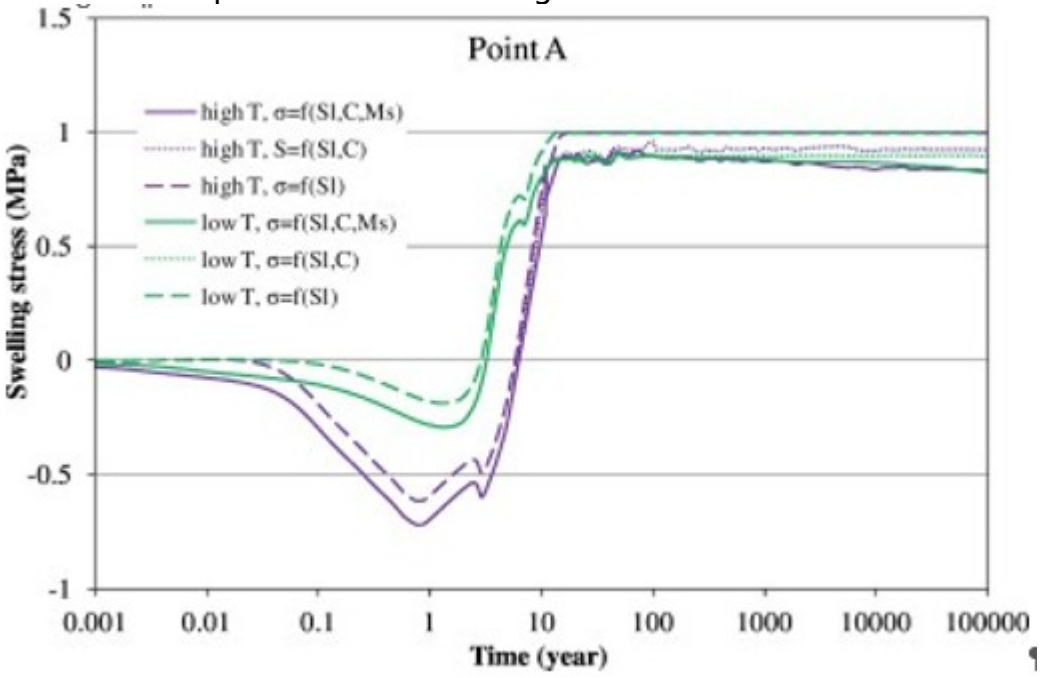

Fig. 8. Simulation results of swelling stress at point A for the “low T” and “high T” scenarios, respectively.

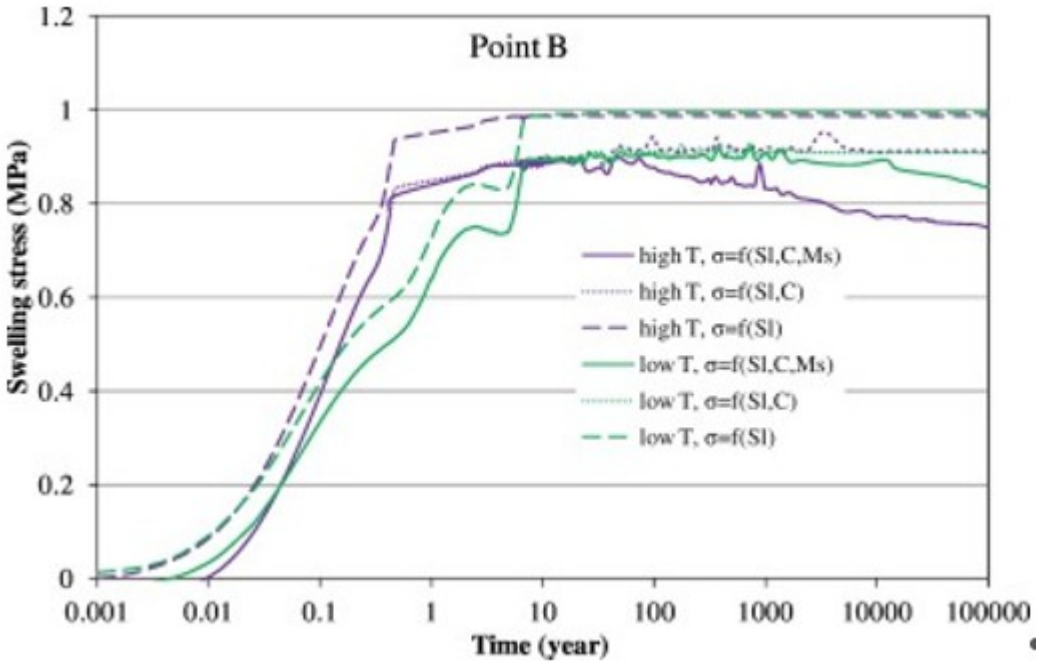

Fig. 9. Simulation results of swelling stress at point B for the “low T” and “high T” scenarios, respectively.

At point A, for the “low T’ case, the ion concentration increase leads to a drop in swelling stress of about 0.11 MPa and the dissolution of smectite reduces the swelling stress a little further by about 0.06 MPa after 100,000 years. For the “high T” case, ion concentration changes cause about a 0.08 MPa decrease in swelling stress and the loss of smectite due to dissolution results in about a 0.09 MPa reduction of swelling stress after 100,000 years. In general, the chemical changes in bentonite have a fairly moderate effect on swelling stress, with about 17% swelling stress reduction being due to chemical change for the “low T” and “high T” cases at point A (Fig. 8). In terms of the effect of ion concentration change on swelling stress, bentonite near the bentonite-argillite interface (point B) behaves similarly to bentonite near the canister. After 100,000 years, the ion concentration increase leads to a drop in swelling stress of about 0.1 MPa in both “low T’ and “high T” cases. In terms of the effect of smectite dissolution on the reduction in swelling stress, bentonite near the bentonite-argillite (point B) interface behaves similarly to those near the canister (point A) for the “low T” case, but not for the “high T” case. The chemical changes in bentonite lead to about 54% swelling stress reduction “high T” case (see Fig. 9), which is much higher than the 17% swelling stress reduction at point B for the “low

T” case. This is caused by more dissolution of smectite in bentonite near bentonite-argillite interface (see Fig. 4 at point B) for the “high T” case. In terms of the total stress, the decrease of swelling stress accounts for about a 3–10% reduction of the total stress after 100,000 years.

The mechanical model for argillite is also linked to the chemical changes with a similar coupling scheme to that used for bentonite, which provides an opportunity to check the effect of chemical change in the argillite on stress. In the “high T” case the effect of ion concentration and smectite change on stress are considered. We developed two sensitivity runs in which the contribution of ion concentration and smectite volume fraction change to stress are alternatively neglected to check on the contribution of chemical changes on the stress. The “high T, no Sc” case in which the contribution of smectite change to stress is neglected and the “high T, no C, no Sc” case in which both the contribution of smectite change and ion concentration to stress is neglected, are shown in Fig. 10. Model results for these three cases show that the effects on stress are very small. By the end of 100,000 years at point C, the dissolution of smectite leads to a decrease in stress of about 0.14 MPa and ion concentration change cause another decrease in stress of about 0.14 MPa. Therefore, in total, the chemical changes in the argillite result in about a 0.28 MPa decrease in stress, or 2.6%. For locations deeper into the argillite, chemical changes account for only about a 0.1 MPa difference in stress (results are not shown).

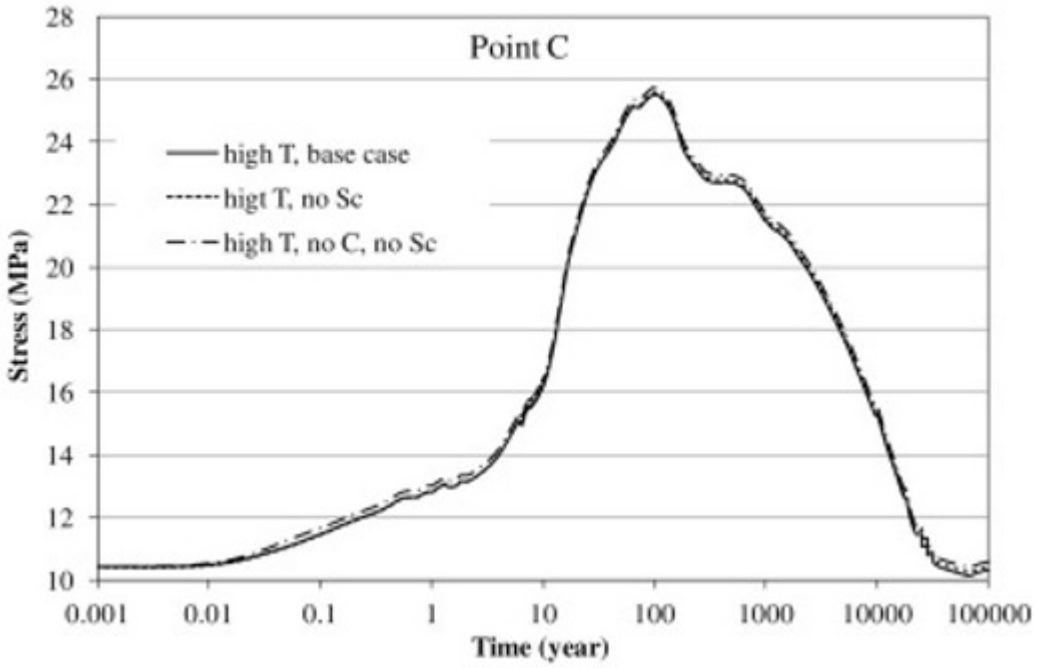

Fig. 10. Simulation results of mean total stress at point C for the “high T” scenarios in three cases: the ‘high T, base case” in which the effect ion concentration and smectitechange on stress are considered; the “high T, no Sc” case in which the contribution of smectite change to stress is neglected and the “high T, no C, no Sc” case in which both the contribution of smectite change and ion concentration to stress are neglected.

4.2. Cases for FEBEX bentonite

In order to understand the change in THMC properties under high temperature for different type of bentonite, models were also developed for FEBEX bentonite as an alternative to Kunigel-VI bentonite discussed in Section 4.1. Kunigel-VI bentonite (Ochs et al., 2004) represents a bentonite type having low smectite content and relative low swelling capacity, whereas FEBEX bentonite (ENRESA, 2000) represents a type of bentonite having high fraction of smectite and high swelling capacity. MX-80 bentonite (Herbert et al., 2008) is somewhere in between in terms of the smectite content and swelling capacity. FEBEX bentonite differs from the Kunigel-VI bentonite in the following aspects:

1. In terms of aqueous chemistry, FEBEX bentonite has higher ion concentration in pore water than Kunigel-VI bentonite, as shown in Table 2. The concentration of major cations, i.e., Ca, Mg, Na, K for FEBEX bentonite is about 2 orders of magnitude higher than that for Kunigel-VI bentonite, which could affect the illitization over the course of heating and hydration.

2. In terms of mineralogical composition, the most pronounced and relevant difference between FEBEX and Kunigel-VI bentonite is the content of smectite, with FEBEX bentonite containing about 60 vol% smectite and Kunigel-VI bentonite having only about 31 vol% smectite (see Table 1). FEBEX bentonite has also less K-feldspar, which could affect illitization.
3. FEBEX bentonite also has higher swelling capacity (in terms of maximum swelling pressure), ranging from 4.5 MPa (Castellanos et al., 2008) to 7 MPa (ENRESA, 2000), than Kunigel-VI bentonite, which has swelling pressure of around 1 MPa (Börgesson et al., 2001, Komine and Ogata, 1996) measured using distilled water. Therefore, the β_{SW} in Eq. (3) for FEBEX bentonite is 0.238 (Rutqvist et al., 2011), which is higher than that used for Kunigel-VI bentonite (0.048).
4. Another difference between FEBEX and Kunigel-VI bentonite is the parameter A_{sc} that relates swelling stress to the abundance of smectite. For FEBEX bentonite, as shown in Fig. 3, a linear regression curve is taken across the FEBEX bentonite, which give us a slope (A_{sc}) of 6.5E + 6 Pa that is higher than the 2.5E + 6 Pa used for Kunigel-VI bentonite.

4.2.1. Chemical evolution

In order to delineate the effect of differences in chemical and mechanical properties on the long term chemical changes and the subsequent mechanical changes, the same thermal conductivity and permeability are used for FEBEX bentonite as used for Kunigel-VI bentonite. The temperature and water saturation for FEBEX bentonite are therefore the same as presented in Section 4.1.1. Changes in smectite volume fractions are shown in Fig. 11. An examination of the model results for Kunigel-VI and FEBEX bentonite reveals that some changes are common to both bentonites and some are distinct. Some common observations for both bentonites are as follows:
– Illitization occurs in bentonite and is enhanced at higher temperature.
– Bentonite near the bentonite-argillite interface undergoes more illitization than that near the waste package.
– Starting from about 1600 years for the “high T” case, coincident with the time that smectite is depleted and illitization ceases in the argillite near the bentonite-argillite interface, the dissolution of smectite is accelerated.

– In the far field of the argillite (e.g. point D), it takes about 3400 years to transform all smectite to illite for the “high T” case, but there is still 60% left after 100,000 years for the “low T” case.

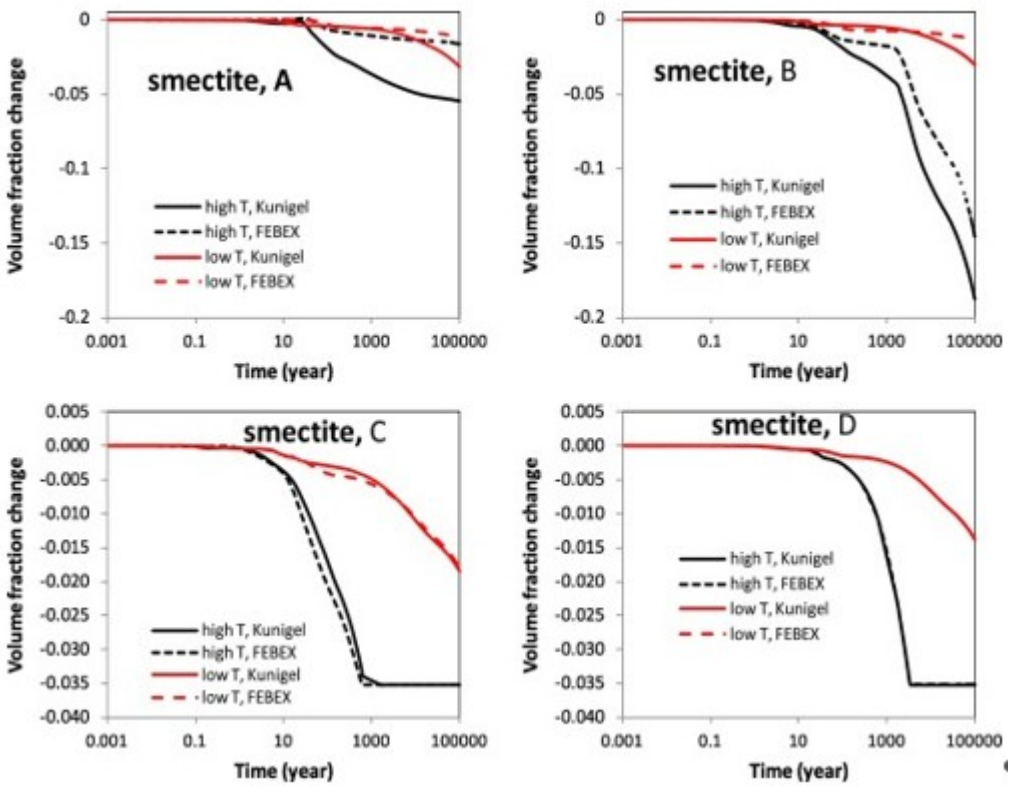

Fig. 11. The temporal evolution of smectite volume fraction at points A, B, C, and D for Kunigel and FEBEX bentonite.

However, in comparison with the model results for Kunigel-VI bentonite, several distinct features have been observed for FEBEX bentonite.

– There is less smectite dissolution for FEBEX bentonite for both “high T” and “low T” scenarios after 100,000 years. For the “high T” case, smectite volume fraction decreases about 0.03 at point A and 0.14 at point B, about 5% and 23% of the initial smectite volume fraction, respectively. These changes are lower than a decrease of 0.05 (17% of initial amount) at point A and 0.19 (60% of the initial amount) for Kunigel-VI bentonite.
– The enhancement of illitization (expressed as smectite dissolution and illite dissolution) by temperature is less pronounced for FEBEX, i.e. the difference between the amount of smectite dissolving for the “low T” and “high T’

scenarios is less significant for FEBEX bentonite than for Kunigel-VI bentonite.
– Although the different types of EBS bentonite have almost no impact on the chemical changes in the argillite away from the bentonite-argillite interface (illustrated by results at point D in Fig. 13), the type of bentonite does have a moderate impact on the argillite near the EBS bentonite. As shown by the results at point C in Fig. 13, with FEBEX bentonite, smectite dissolution occurs earlier in the argillite. The reason is that FEBEX bentonite has a higher K concentration (see Table 2) so that the diffusion of K from the argillite into the bentonite is at lower rate, and subsequently more K is available in the argillite for illitization.

4.2.2. Stress evolution

Fig. 12, Fig. 13 show the stress changes in the sensitivity run using FEBEX bentonite at points A and B for both “low T” and “high T” cases. As discussed in Section 4.1.2, the increase in pore pressure due to hydration and thermal pressurization, bentonite swelling, and thermal expansion are the main driving force for the increase in total stress in bentonite. In comparison with the “low T” case, the stronger thermal pressurization in the “high T” case clearly leads to much higher stress in the bentonite. For both the “high T” and “low T” cases, the major contribution to the total stress within the buffer is from pore pressure, with smaller contributions from swelling and thermal stress. As observed for Kunigel-VI bentonite, the stress peak occurs at around 100 years and then decreases thereafter. After 20,000 to 30,000 years, the stress seems to reach a stable state.

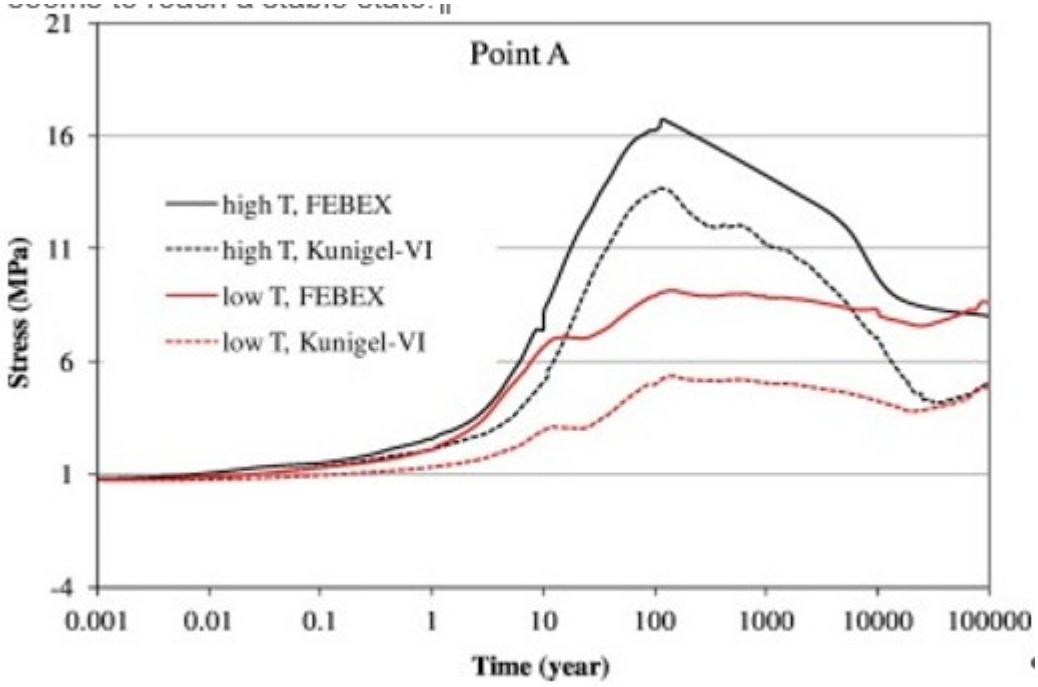

Fig. 12. Simulation results of mean total stress at point A for Kunigel-VI and FEBEX bentonite for the "low T" and "high T" scenarios, respectively.

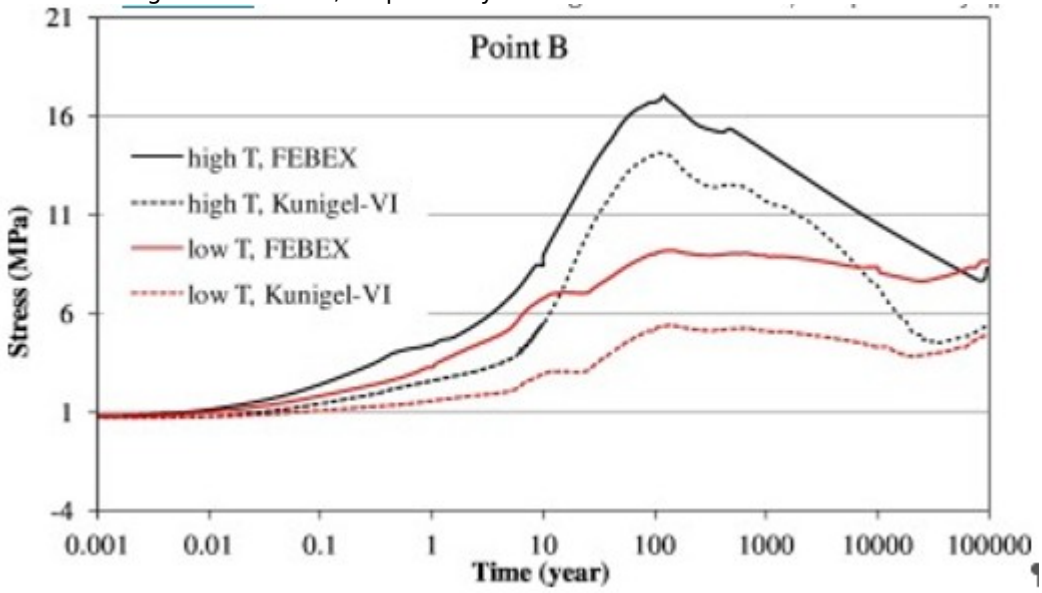

Fig. 13. Simulation results of mean total stress at point B for Kunigel-VI and FEBEX bentonite for the "low T" and "high T" scenarios, respectively.

Fig. 12, Fig. 13 compare the total stress calculated for the Kunigel-VI and FEBEX bentonite. Because FEBEX bentonite has higher swelling pressure, the total stress for FEBEX bentonite at points A and B are 3–4 MPa higher than that for Kunigel bentonite at the peak (100 years) and this difference persists until the end of the simulation at 100,000 years.

The constitutive relationship described by Eq. (5) shows that the swelling stress changes have contributions from moisture, ion concentration and smectite changes. The same as to what has been done for the Kunigel-VI bentonite, we also present three sets of calculated swelling stresses for FEBEX bentonite to delineate the contribution from each process by alternatively neglecting the contribution of smectite (Ms) (case “σ = f(Sl,C)” in Fig. 14, Fig. 15) to swelling stress, or the contribution of both ion concentration (C) changes and smectite (Ms) to swelling stress (case “σ = f(Sl)” in Fig. 14, Fig. 15). At point A near the canister, pore water in the bentonite evaporates causing the liquid saturation to decrease. This results in a decrease of swelling stress (shrinkage) until about 4 years for “low T” scenario and 8 years for “high T” scenario (Fig. 14). After that, increases in liquid saturation induce swelling and swelling stress keeps increasing until reaching the swelling capacity of 5 MPa. In comparison with the swelling stress for Kunigel-VI bentonite at point A (presented in Section 4.1.2), the swelling stress for FEBEX bentonite has two distinct features. First, ion concentration has a minimal effect on the swelling stress because the ion concentration of the pore water in FEBEX bentonite is fairly close to that in the argillite. Second, a greater stress reduction due to smectite dissolution has been observed for FEBEX bentonite. Despite that, less smectite dissolution has been observed for FEBEX bentonite (Fig. 11) and a higher A_{sc} (a parameter that relates swelling stress with the abundance of smectite) for FEBEX bentonite leads to slightly higher reduction in swelling stress. Table 4 lists the stress reduction by ion concentration and smectite dissolution at point A for Kunigel-VI and FEBEX bentonites. In total, chemical changes leads to about 0.17 MPa stress decrease for Kunigel-VI bentonite and 0.18 MPa for FEBEX bentonite. In comparison with the swelling stress obtained with “σ = f(Sl)”, chemical change causes about 16% reduction in swelling stress for Kunigel-VI bentonite, but only 3.4% for FEBEX bentonite.

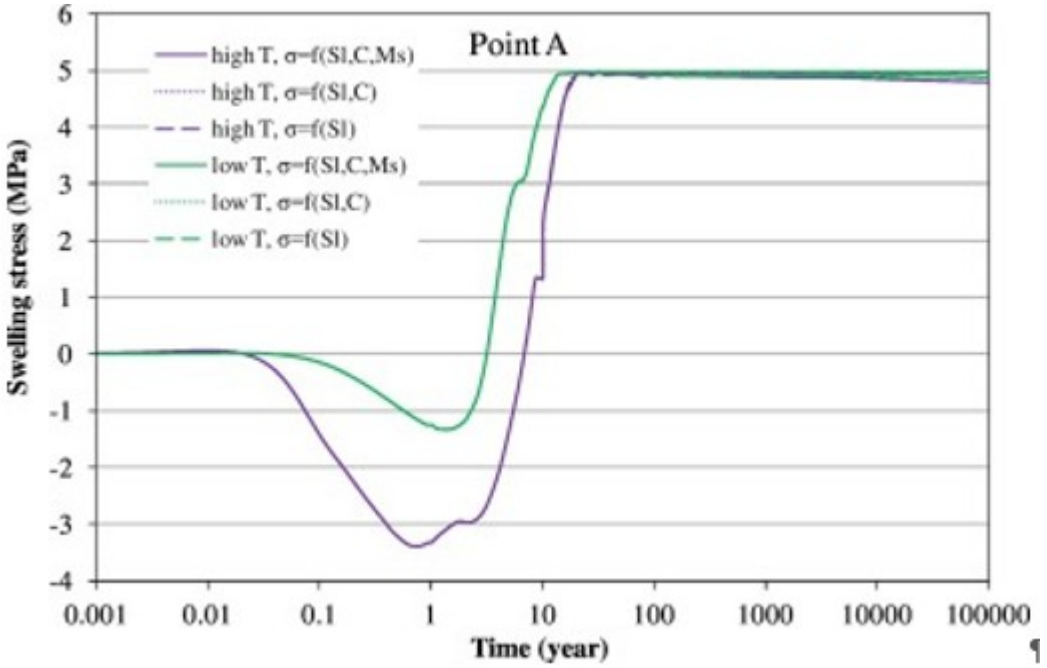

Fig. 14. Simulation results of swelling stress at point A for the FEBEX bentonite for the “low T” and “high T” scenarios, respectively, focusing on the stress range from 4.5 to 5 MPa.

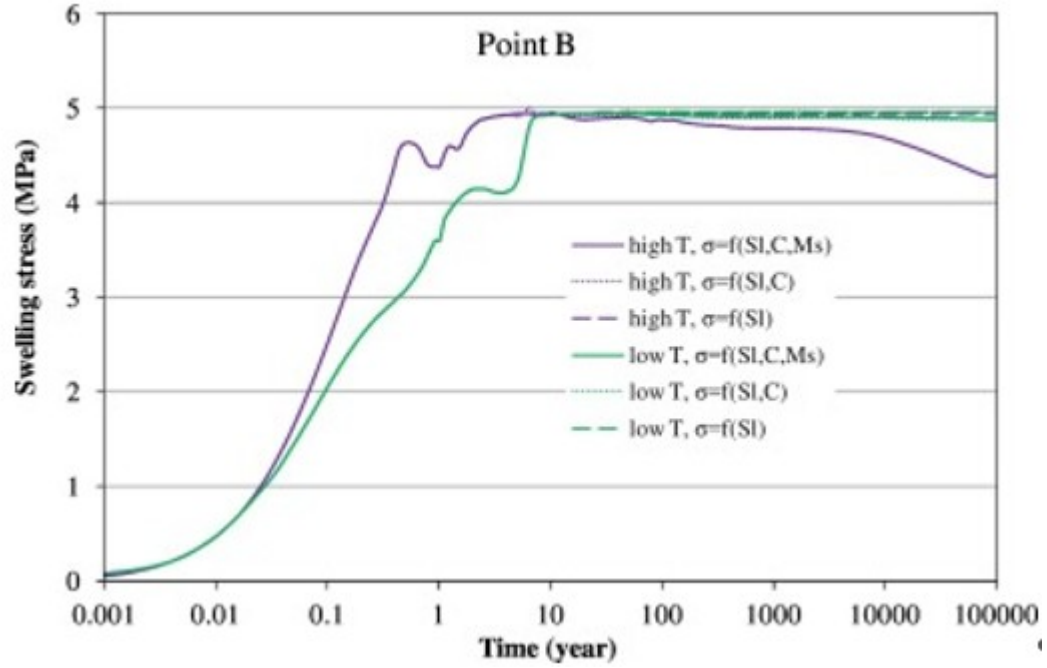

Fig. 15. Simulation results of swelling stress at point B for the FEBEX bentonite for the “low T” and “high T” scenarios, respectively, focusing on the stress range from 4.5 to 5 MPa.

Table 4. The geochemically induced swelling stress for Kunigel and FEBEX bentonite at points A and B for “high T” scenario. Stress reduction by ion concentration is the difference between the swelling stress obtained with “σ = f(Sl)” and “σ = f(Sl,C)”, and the stress reduction

by smectite dissolution is the difference between the swelling stress obtained with “σ = f(Sl,C)” and “σ = f(Sl,C,Ms)” (see Fig. 14, Fig. 15), where the relative amount (%) use the results from “σ = f(Sl)” as the basis.

	Kunigel-VI bentonite				FEBEX bentonite			
	Stress reduction by ion concentration		Stress reduction by smectite dissolution		Stress reduction by ion concentration		Stress reduction by smectite dissolution	
	MPa	%	MPa	%	MPa	%	MPa	%
Point A	0.07	7%	0.09	9%	0.006	0.1%	0.17	3.4%
Point B	0.08	8%	0.45	45%	0.06	1.1%	0.6	12%

Model results at point B (Fig. 15) lead to the same observation in terms of the difference between Kunigel-VI and FEBEX bentonite, although the specific values differ significantly from those at point A. As we discussed in the previous section, because of the interaction between bentonite and the argillite, bentonite near the interface goes through further dissolution of smectite after about 20,000–30,000 years when the dissolution of smectite in bentonite near the waste package become stable, which lead to further decrease in swelling stress. By the end of 100,000 years, as illustrated in Fig. 15 and articulated in Table 4, Kunigel-VI bentonite has lost more than half of its swelling capacity whereas FEBEX bentonite has lost about 13% of its swelling capacity. Generally speaking, in absolute numbers, Kunigel-VI and FEBEX bentonites undergo similar magnitudes of reduction in swelling stress, but relative to their swelling capacity (the maximum swelling stress which is typically measured by hydrating bentonite with deionized water), chemical changes cause a stronger reduction in swelling capacity for Kunigel-VI than for FEBEX bentonite. Therefore, using bentonite with a high swelling capacity such as FEBEX bentonite is always beneficial with respect to stress reduction caused by illitization.

5. Discussion and conclusions

This study investigates the impact of strongly elevated temperature on the bentonite backfill and near-field clay host rock in a geologic repository

for radioactive waste. We use coupled THMC modeling to evaluate the chemical alteration and associated mechanical changes in a generic repository and consider the interaction between EBS bentonite and the argillite. Two main scenarios were developed for comparison: a “high T” case in which the temperature near the waste package reaches about 200 °C, and a “low T” scenario in which the temperature peaks at about 100 °C.

In this paper, our previous model simulations, with EBS properties based on Kunigel-VI bentonite (Zheng et al., 2015), was extended from 1000 years to 100,000 years. Meanwhile, a THMC model with EBS properties based on FEBEX bentonite were also developed to evaluate how different types of bentonite behave in terms of illitization and subsequent stress change under high temperature.

Our model results for 100,000 years confirm some findings from the previous 1000-year simulations (Liu et al., 2013, Zheng et al., 2015). There is some degree of illitization in the EBS bentonite and argillite and illitization is enhanced under higher temperature. However, the present 100,000-year simulations also lead to some distinct observations regarding illitization in comparison with that in Zheng et al. (2015), especially for the high temperature condition:

– Model results reveals that for the “high T” scenario, illitization is stabilized after about 2000 years in bentonite near the waste package, but continues in bentonite near the bentonite-argillite interface. For the “low T’ scenario, illitization is nearly stabilized after 2000 years for the entire volume of EBS bentonite.

– The geochemical interaction between EBS bentonite and the argillite has a strong effect on long term illitization in bentonite. Previous simulations, namely the 1000-years simulations in Zheng et al. (2015), showed that illitization reactions in bentonite are tied to the dissolution rate of K-feldspar that occurs locally, and as a result, illitization is fairly homogeneous in the entire bentonite barrier. However, the 100,000-year simulations show that bentonite near the bentonite-argillite interface undergo more illitization than that near the waste package by the end of 100,000 years for the “high T’ scenarios. The reason is that after 2000–3000 years, the illitization process ceases in the argillite and the K ion is not consumed by the local illitization

and is, therefore, transported into the EBS bentonite to facilitate further illitization.

In terms of the effect of chemical changes on swelling stress for bentonite, the current modeling results show a more significant reduction in swelling stress as a result of smectite dissolution after 100,000 years than previously revealed by the 1000-years simulations. This is particularly true for bentonite near the bentonite-argillite interface as illitization continues in these areas. For the “high T” case, Kunigel-VI bentonite near the bentonite-argillite loses as much as 53% swelling capacity and FEBEX bentonite near the EBS-NS has about 13% reduction in swelling stress, whereas bentonite near the waste package undergoes a small reduction in swelling stress — 16% reduction for Kunigel-VI and 3.4% for FEBEX bentonite, respectively. For the “low T” case, the stress reduction by chemical change is relatively homogeneous, 16% reduction for Kunigel-VI bentonite and around 3% reduction for FEBEX bentonite after 100,000 years.

Chemical effects were incorporated in the mechanical model for the argillite and the effect of chemical change in argillite on the total stress was evaluated. Chemical change leads to about a 2.6% decrease in stress near the bentonite-argillite interface and about 0.7% in the far field. In general, chemical change does not have significant impact on the stress in the argillite.

As mentioned in the beginning of the paper, a thermal limit of about 100 °C is imposed in most disposal concepts throughout the world—without rigorous studies to back up the choice. The THMC simulations here were conducted to trying to shed light on whether an argillite repository with a bentonite-based EBS can sustain higher than 100 °C. While this modeling exercise improves understanding of the coupled processes that contribute to chemical and mechanical alteration in the EBS bentonite and argillite, the results should be interpreted cautiously because of the limitations and assumptions in the model. However, current and previous the modeling work (Liu et al., 2013, Zheng et al., 2015) leads to a tentative conclusion that a clay repository with bentonite EBS could sustain higher than 100 °C as far as illitization concerns, with the following cautious remarks:

1. The thermal limit has to be evaluated case by case, as manifested by the fact that Kunigel-VI and FEBEX bentonite behave distinctively in terms of illitization and its effect on swelling stress.

2. Provided that illitization causes a decrease of swelling pressure and thus compromise the functionality of EBS such sealing the gap, using bentonite with high swelling capacity (e.g., FEBEX bentonite) or emplaced at a higher dry-density will greatly ease such issue.

Acknowledgments

Funding for this work was provided by the Spent Fuel and Waste Science and Technology, Office of Nuclear Energy, of the U.S. Department of Energy under Contract Number DE-AC02-05CH11231 with Lawrence Berkeley National Laboratory.

References

Alonso et al., 1999
E.E. Alonso, J. Vaunat, A. Gens**Modeling the mechanical behaviour of expansive clays**
Eng. Geol., 54 (1999), pp. 173-183
Börgesson et al., 2001
L. Börgesson, M. Chijimatsu, T.S. Nguyen, J. Rutqvist, L. Jing**Thermo-hydro-mechanical characterization of a bentonite-based buffer material by laboratory tests and numerical back analyses**
Int. J. Rock Mech. Min. Sci., 38 (2001), pp. 105-127
Bossart, 2011
P. Bossart**Characteristics of the Opalinus Clay at Mont Terri**
http://www.mont-terri.ch/internet/mont-terri/en/home/geology/key_characteristics.html(2011)
Castellanos et al., 2008
E. Castellanos, M.V. Villar, E. Romero, A. Lloret, A. Gens**Chemical impact on the hydro-mechanical behaviour of high-density FEBEX bentonite**
Phys. Chem. Earth Parts A/B/C, 33 (Supplement 1(0)) (2008), pp. S516-S526
Chen et al., 2009
Y. Chen, C. Zhou, L. Jing**Modeling coupled THM processes of geological porous media with multiphase flow: theory and validation against laboratory and field scale experiments**
Comput. Geotech., 36 (8) (2009), pp. 1308-1329
Cuadros and Linares, 1996
J. Cuadros, J. Linares**Experimental kinetic study of the smectite-to-illite transformation**
Geochim. Cosmochim. Acta, 60 (3) (1996), pp. 439-453

ENRESA, 2000
ENRESA**Full-scale engineered barriers experiment for a deep geological repository in crystalline host rock FEBEX Project**
European Commission (2000), p. 403
Fernández et al., 2001
A. Fernández, J. Cuevas, P. Rivas**Pore water chemistry of the FEBEX bentonite**
Mat. Res. Soc. Symp. Proc., 663 (2001), pp. 573-588
Fernández et al., 2004
A.M. Fernández, B. Baeyens, M. Bradbury, P. Rivas**Analysis of the porewater chemical composition of a Spanish compacted bentonite used in an engineered barrier**
Phys. Chem. Earth Parts A/B/C, 29 (1) (2004), pp. 105-118
Fernández et al., 2007
A.M. Fernández, M.J. Turrero, D.M. Sánchez, A. Yllera, A.M. Melón, M.Sánchez, J. Peña, A. Garralón, P. Rivas, P. Bossart, P. Hernán**On site measurements of the redox and carbonate system parameters in the low-permeability Opalinus Argillite at the Mont Terri Rock Laboratory**
Phys. Chem. Earth Parts A/B/C, 32 (1–7) (2007), pp. 181-195
Gaston et al., 2009
D. Gaston, C. Newman, G. Hansen, D. Lebrun-Grandie**MOOSE: a parallel computational framework for coupled systems of nonlinear equations**
Nucl. Eng. Des., 239 (10) (2009), pp. 1768-1778
Gens et al., 2004
A. Gens, L.D.N. Guimarães, S. Olivella, M. Sánchez**Analysis of the Thmc Behaviour of Compacted Swelling Clay for Radioactive Waste Isolation**
Elsevier Geo-Engineering Book Series, 2, Elsevier, S. Ove (2004), pp. 317-322
Guimarães et al., 2007
L.D.N. Guimarães, A. Gens, S. Olivella**Coupled thermo-hydro-mechanical and chemical analysis of expansive clay subjected to heating and hydration**
Transp. Porous Media, 66 (3) (2007), pp. 341-372
Guimarães et al., 2013
L.D.N. Guimarães, A. Gens, M. Sánchez, S. Olivella**A chemo-mechanical constitutive model accounting for cation exchange in expansive clays**
Géotechnique, 63 (2013), pp. 221-234

Herbert et al., 2008
H.J. Herbert, J. Kasbohm, H. Sprenger, A.M. Fernández, C. Reichelt**Swelling pressures of MX-80 bentonite in solutions of different ionic strength**
Phys. Chem. Earth Parts A/B/C, 33 (Supplement 1(0)) (2008), pp. S327-S342
Hicks et al., 2009
T.W. Hicks, M.J. White, P.J. Hooker**Role of Bentonite in Determination of Thermal Limits on Geological Disposal Facility Design, Report 0883-1, Version 2**
Falson Sciences Ltd., Rutland, UK (2009)
(Sept. 2009)
Horseman and McEwen, 1996
S.T. Horseman, T.J. McEwen**Thermal constrains on disposal of heat-emitting waste in argillaceous rocks**
Eng. Geol., 41 (1996), pp. 5-16
Kim et al., 2015
J. Kim, E. Sonnenthal, J. Rutqvist**A sequential implicit algorithm if chemo-thermo-poro-mechanics for fractured geothermal reservoir**
Comput. Geosci., 76 (2015), pp. 59-71
Komine and Ogata, 1996
H. Komine, N. Ogata**Prediction for swelling characteristics of compacted bentonite**
Can. Geotech. J., 33 (1996), pp. 11-22
Laredj et al., 2010
N. Laredj, H. Missoum, K. Bendani**Modeling the effect of osmotic potential changes on deformation behavior of swelling clays**
J. Porous Media, 13 (8) (2010), pp. 743-748
Lauber et al., 2000
M. Lauber, B. Baeyens, M.H. Bradbury**Physico-Chemical Characterisation and Sorption Measurements of Cs, Sr, Ni, Eu, Th, Sn and Se on Opalinus Clay from Mont Terri**
(2000)
(PSI Bericht Nr. 00-10 December 2000 ISSN 10190643)
Liu et al., 2013
H.H. Liu, J. Houseworth, J. Rutqvist, L. Zheng, D.E. Asahina, V. Li Vilarrasa, F.Chen, S. Nakagawa, S. Finsterle, C. Doughty, T. Kneafsey, J. Birkholzer**Report on THMC Modeling of the Near Field Evolution of a Generic Clay Repository, Model Validation and Demonstration**
Lawrence Berkeley National Laboratory (2013)
(August, 2013, FCRD-UFD-2013-0000244)

Nguyen et al., 2005
T.S. Nguyen, A.P.S. Selvadurai, G. Armand**Modelling the FEBEX THM experiment using a state surface approach**
International Journal of Rock Mechanics and Mining Science, 42 (5–6) (2005), pp. 639-651
Ochs et al., 2004
M. Ochs, B. Lothenbach, M. Shibata, M. Yui**Thermodynamic modeling and sensitivity analysis of porewater chemistry in compacted bentonite**
Phys. Chem. Earth Parts A/B/C, 29 (1) (2004), pp. 129-136
Pusch and Karnland, 1996
R. Pusch, O. Karnland**Physico/chemical stability of smectite clays**
Eng. Geol., 41 (1996), pp. 73-85
Pusch and Madsen, 1995
R. Pusch, F.T. Madsen**Aspects on the illitization of the kinnekulle bentonites**
Clay Clay Miner., 43 (3) (1995), pp. 261-270
Pusch et al., 2010
R. Pusch, J. Kasbohm, H.T.M. Thao**Chemical stability of montmorillonite buffer clay under repository-like conditions—a synthesis of relevant experimental data**
Appl. Clay Sci., 47 (1–2) (2010), pp. 113-119
Ramírez et al., 2002
S. Ramírez, J. Cuevas, R. Vigil, S. Leguey**Hydrothermal alteration of “La Serrata” bentonite (Almeria, Spain) by alkaline solutions**
Appl. Clay Sci., 21 (5–6) (2002), pp. 257-269
Rutqvist et al., 2011
J. Rutqvist, Y. Ijiri, H. Yamamoto**Implementation of the Barcelona Basic Model into TOUGH-FLAC for simulations of the geomechanical behavior of unsaturated soils**
Comput. Geosci., 37 (2011), pp. 751-762
Rutqvist et al., 2014
J. Rutqvist, L. Zheng, F. Chen, H.H. Liu, J. Birkholzer**Modeling of coupled thermo-hydro-mechanical processes with links to geochemistry associated with bentonite-backfilled repository tunnels in clay formations**
Rock Mech. Rock. Eng., 47 (2014), pp. 167-186
Sánchez et al., 2005
M. Sánchez, A. Gens, L.J.D.N. Guimarães, S. Olivella**A double structure generalized plasticity model for expansive materials**

Int. J. Numer. Anal. Methods Geomech., 29 (2005), pp. 751-787
Sonnenthal, 2008
E. Sonnenthal**Chapter 5**
J. Rutqvist Birkholzer, E. Sonnenthal, D. Barr (Eds.), Long-Term Permeability/Porosity Changes in the EDZ and Near Field due to THM and THC Processes in Volcanic and Crystalline-Bentonite Systems, DECOVALEX-THMC Project Task D Final Report (2008)
Taron et al., 2009
J. Taron, D. Elsworth, K.B. Min**Numerical simulation of thermal–hydrologic–mechani-cal–chemical processes in deformable, fractured porous media**
Int. J. Rock Mech. Min. Sci., 46 (2009), pp. 842-854
Tsang, 2009
C.F. Tsang**Introductory editorial to the special issue on the DECOVALEX-THMC project**
Environ. Geol., 57 (6) (2009), pp. 1217-1219
Wang et al., 2011
W. Wang, J. Rutqvist, U.J. Görke, J.T. Birkholzer, O. Kolditz**Non isothermal flow in low permeable porous media: a comparison of Richards' and two-phase flow approaches**
Environ. Earth Sci., 62 (2011), pp. 1197-1207
Wersin et al., 2007
P. Wersin, L.H. Johnson, I.G. McKinley**Performance of the bentonite barrier at temperature beyond 100°C: a critical review**
Phys. Chem. Earth, 32 (2007)
Xu et al., 2011
T. Xu, N. Spycher, E. Sonnenthal, G. Zhang, L. Zheng, K. Pruess**TOUGHREACT version 2.0: a simulator for subsurface reactive transport under non-isothermal multiphase flow conditions**
Comput. Geosci., 37 (6) (2011), pp. 763-774
Yin et al., 2010
S. Yin, B. Towler, M. Dusseault, L. Rothenburg**Fully coupled THMC modeling of wellbore stability with thermal and solute convection considered**
Transp. Porous Media, 84 (3) (2010), pp. 773-798
Yin et al., 2011
S. Yin, M.B. Dusseault, L. Rothenburg**Coupled THMC modeling of CO_2 injection by finite element methods**
J. Pet. Sci. Eng., 80 (1) (2011), pp. 53-60

Zhang et al., 2012
R. Zhang, X. Yin, P.H. Winterfeld, Y.S. Wu**A fully coupled model of nonisothermal multiphase flow, geomechanics, and chemistry during CO_2 sequestration in brine aquifers**
Proc. Tough Symp. (2012), pp. 838-848
Zheng and Samper, 2008
L. Zheng, J. Samper**A coupled THMC model of FEBEX mock-up test**
Phys. Chem. Earth Parts A/B/C, 33 (Supplement 1) (2008), pp. S486-S498
Zheng et al., 2010
L. Zheng, J. Samper, L. Montenegro, A.M. Fernández**A coupled THMC model of a heating and hydration laboratory experiment in unsaturated compacted FEBEX bentonite**
J. Hydrol., 386 (1–4) (2010), pp. 80-94
Zheng et al., 2011
L. Zheng, J. Samper, L. Montenegro**A coupled THC model of the FEBEX in situ test with bentonite swelling and chemical and thermal osmosis**
J. Contam. Hydrol., 126 (1–2) (2011), pp. 45-60
Zheng et al., 2014
L. Zheng, J. Rutqvist, H.H. Liu, J.T. Birkholzer, E. Sonnenthal**Model evaluation of geochemically induced swelling/shrinkage in argillaceous formations for nuclear waste disposal**
Appl. Clay Sci., 97–98 (2014), pp. 24-32
Zheng et al., 2015
L. Zheng, J. Rutqvist, J.T. Birkholzer, H.H. Liu**On the impact of temperatures up to 200 °C in clay repositories with bentonite engineer barrier systems: a study with coupled thermal, hydrological, chemical, and mechanical modeling**
Eng. Geol., 197 (2015), pp. 278-295